

Supplementary Methods and analysis

Methods

Confocal imaging of living pancreas slices

Functional imaging of living human pancreas slices was done as previously described (1). Briefly, slices were incubated with Fluo4-AM (6.3 μ M, Invitrogen, cat. nr. F14201) and DyLight 649 lectin from *Lycopersicon Esculentum* (final concentration 3.3 μ g/mL, VectorLabs, cat. nr. DL1178) for 1h in 3 mM glucose solution prepared in HEPES buffer (125 mmol/l NaCl, 5.9 mmol/l KCl, 2.56 mmol/l CaCl₂, 1 mmol/l MgCl₂, 25 mmol/l HEPES, 0.1% BSA [w/v], pH 7.4), supplemented with aprotinin (25 KIU, MilliporeSigma, cat. nr. A6106) at room temperature and in the dark. To identify pericytes *in situ*, slices were incubated for 2h with a fluorescent-conjugated antibody against NG2 (final dilution 1:50, R&D Systems, cat. nr. Fab2585R). After incubation, living pancreas slices were placed on a coverslip in an imaging chamber (Warner instruments, Hamden, CT, USA) and imaged under an upright confocal microscope (Leica TCS SP5 upright; Leica Microsystems, Wetzlar, Germany). The chamber was continuously perfused with HEPES-buffered solution containing 3 mM glucose and confocal images were acquired with LAS AF software (Leica Microsystems) using a 40X water immersion objective (NA 0.8). We used a resonance scanner for fast image acquisition to produce time-lapse recordings spanning 50-100 μ m of the slice (z-step: 5-10 μ m, stack of 10-15 confocal images with a size of 512 \times 512 pixels) at 5 seconds resolution (xyzt imaging). Fluo-4 fluorescence was excited at 488 nm and emission detected at 510–550 nm, DyLight 649 labeled tomato lectin was excited at 638 nm and emission detected at 648-690 nm.

From each human donor, a group of slices was incubated with Fluo4 and lectin and another group of slices was incubated with Fluo4 and NG2-alexa647, to account for potential effects of antibody binding and change in cell physiology. Mural cells responded similarly with or without antibody labeling.

We recorded changes in [Ca²⁺]_i and blood vessel diameter induced by norepinephrine (20 μ M), endothelin-1 (10 nM). To quantify changes in [Ca²⁺]_i, we drew regions of interest around individual islet pericytes and measured the mean Fluo4 fluorescence intensity using ImageJ software (<http://imagej.nih.gov/ij/>). Changes in

fluorescence intensity were expressed as percentage over baseline ($\Delta F/F$). The baseline was defined as the mean of the three first values of the control period of each recording [i.e., in non-stimulatory, basal glucose concentration conditions (3 mM)]. Heatmaps showing relative changes in fluorescence for individual pericytes were generated in MatLab.

Blood vessels were labeled with DyLight-649 and we could image vessel borders in slices. Quantification of vessel diameter was done as previously described (2). Briefly, we drew a straight-line transversal to the blood vessel borders and used the “reslice” z-function in ImageJ to generate a single image showing the changes in vessel diameter over time (xt scan; temporal projection). We drew another line on the xt scan (resliced) image and, using the “plot profile” function, we determined the position of the pixels with the highest fluorescence intensity and considered these the vessel borders. Vessel diameter was calculated by subtracting these 2 position values. To determine the extent of constriction, we pooled data on responsive capillaries from different islets from different donors and calculated the relative change in diameter (as fraction of initial vessel diameter).

Transplantation into the anterior chamber of the eye

Recipient mice were rendered diabetic before islet transplantation with a single intravenous injection of the beta cell toxin streptozotocin (STZ 200 mg/Kg; Sigma, MO) dissolved fresh in 100 mM sodium citrate (pH 4.5) immediately before injection. There was no morbidity or mortality associated with streptozotocin toxicity.

Transplantation into the anterior chamber of the eye was performed as previously described (3, 4). Eyes were kept humidified (ophthalmologic eye drops) to avoid drying of the cornea. Under a stereomicroscope, the cornea was punctured close to the sclera at the bottom part of the eye with a 31G insulin needle. Using the needle, we made a small radial incision of approximately the size of the eye cannula (~ 0.5 mm). For this incision, the needle was barely introduced into the anterior chamber, thus avoiding damage to the iris and bleeding. The blunt eye cannula was then gently inserted through this incision, first perpendicular to the surface of the cornea and then parallel to the cornea. Once the cannula was stably inserted into the eye, the islets were slowly

injected in a 10- μ l volume of sterile saline solution into the anterior chamber, where they settle on the iris. After injection, the cannula was carefully and slowly withdrawn (1 min) to avoid islets from flowing back through the incision. The mouse was left lying on the side before awakening. Mice were then put back in the cages and monitored until full recovery. Analgesia was obtained after surgical procedures with buprenorphine (0.05-0.1 mg/kg s.c.).

Only animals with non-fasting glycemic values >450 mg/dl were transplanted. We transplanted 200 mouse islet equivalents from NG2-ChR2⁺ and NG2-ChR2⁻ mice into the anterior chamber of the right eye of diabetic Nude recipient mice (for optogenetic manipulation) and from C57BL6 mice into diabetic B6 siblings (for pharmacological manipulation with phenylephrine eye drops). This provided an optimal beta cell mass that allowed reversal of diabetes for 26 mice out of 28 recipient mice (total number of transplanted mice for both manipulations) within 1 month after transplantation. The 2 animals that never recovered from diabetes received NG2-ChR2⁺ islets (see Supplementary Fig. 2) and were not included in the study. We defined normoglycemia as 3 consecutive readings of non-fasting blood glucose below 200 mg/dl (2, 4, 5).

In vivo imaging of the mouse eye

Imaging of islets *in vivo* in the anterior chamber of transplanted animals was performed as previously reported. Briefly, mice were anesthetized with ~2% isoflurane air mixture, placed on a heating pad and the head restrained with a headholder. The eyelid was carefully pulled back and the eye gently supported. For fluorescence confocal imaging, an upright SP5 Leica confocal microscope (Leica Microsystems, Mannheim, Germany) was used for imaging together with long distance water-dipping lenses (Leica HXC APO 20x 0.5 W), using Viscotears (Novartis, Basel, Switzerland) as an immersion liquid. ChR2-tdTomato expressing pericytes were visualized upon excitation with 561 nm laser and endocrine cells in islet grafts were imaged by illumination at 633 nm and collection between 630-639 nm. To activate/deactivate ChR2, we turned on/off the 488 nm laser during image acquisition (100% laser power). Blood vessels were labeled by tail vein injection of 150,000 Da Dextran-FITC. FITC was excited at 488 nm and emission light was collected between 500-550 nm. For monitoring the uptake of glucose analog, 2-(N-

(7-Nitrobenz-2-oxa-1,3-diazol-4-yl)Amino)-2-Deoxyglucose (2-NBDG, Thermo Fisher Scientific, USA) was dissolved in saline solution at 5 mg/ml. 100 μ l 2-NBDG solution was injected i.v. Time series of z-stacks (2 μ m) were acquired every 5 sec.

Data analysis was performed with ImageJ (<http://imagej.nih.gov/ij/>; NIH, USA) software. The density of FITC-labeled blood vessels in each islet graft was quantified by calculating the area of stained blood vessels as a fraction of the islet area (vessel density). Changes in capillary diameter induced by optogenetic manipulation of pericytes were determined as described above for experiments with living pancreas slices. To estimate changes in blood flow, we used the “Stack Difference” plugin to detect dynamic pixel changes that correspond to the movement of red blood cells [RBCs; (5)]. We drew regions of interest on different vessels in islet grafts and quantified changes in fluorescence in those regions over time (Supplementary Fig. 6). To estimate RBC fluxes, we calculated the area under the curve of fluorescence traces every 5s after turning on the 488 nm laser, which reflects the total amount of RBCs flowing during that period, and divided it by 5.

Assessment of tissue hypoxia and nitric oxide production

Transplanted mice were placed in the dark and stimulated with pulsed blue light (4 min off, 1 min on) for 4h. The oxygenation marker pimonidazole (60 mg/Kg; dissolved in sterile saline solution; HypoxyprobeTM kit) was injected i.v. 90 min before sacrifice. Pimonidazole that precipitates at oxygen levels of ≤ 8 mmHg (6). Control animals included mice with intraocular NG2-ChR2- islet grafts stimulated with blue light and treated with pimonidazole, and mice with NG2-ChR2+ islet grafts either not stimulated with pulsed blue light or treated with saline solution. After 90 min, animals were sacrificed and the eyes with islet grafts were dissected, fixed in 4% paraformaldehyde (overnight) and processed for immunohistochemistry.

To assess local nitric oxide levels, we used NADPH-diaphorase histochemistry technique. NADPH diaphorase is commonly used as a histochemical marker of nitric oxide synthase and other nitric oxide-containing factors in aldehyde-fixed tissues (7). Briefly, frozen sections of the eyes containing grafts (10 μ m sections) were rinsed twice in 50 mM Tris-buffer (pH 8.0) and incubated for 45 min in Tris-buffer containing 0.5%

Triton X-100, before incubating with nitroblue (0.2 mM) and NADPH (1 mM) at 40°C for 15-30 min. Sections were rinsed, mounted and imaged on a confocal microscope.

Immunohistochemistry

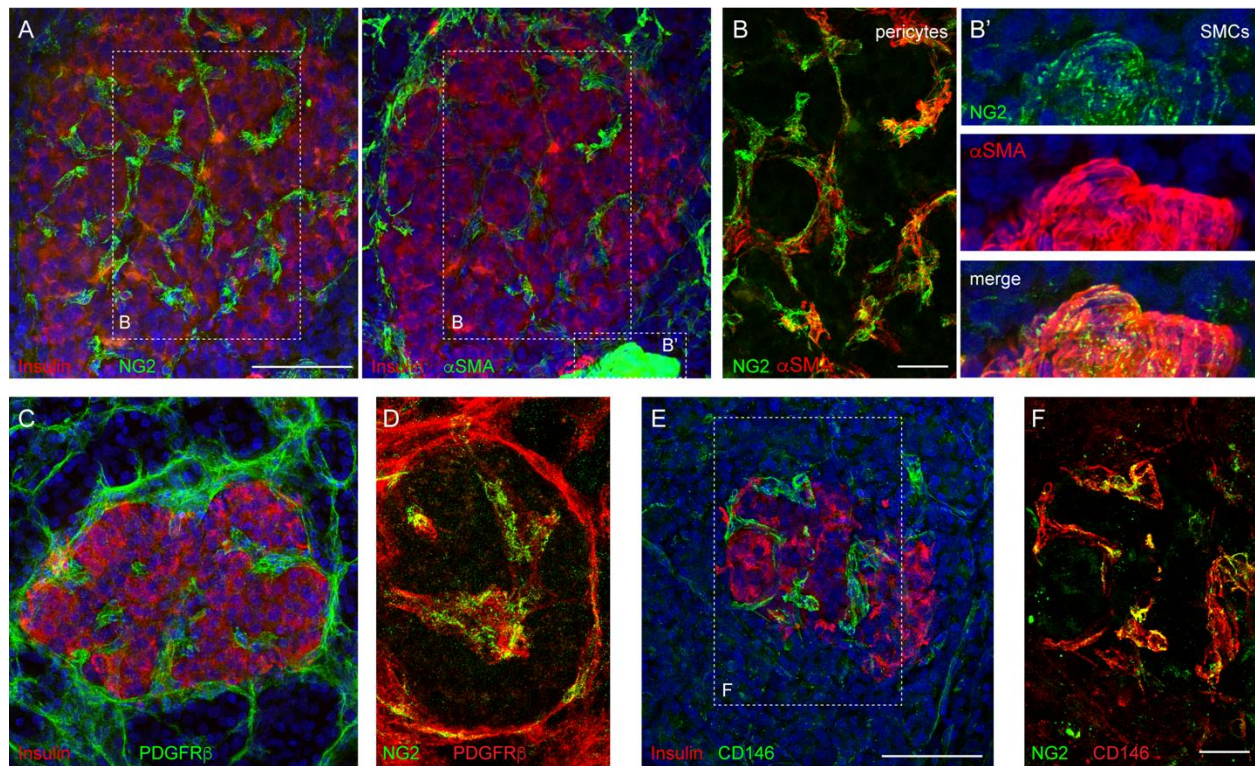
Pancreases and islet grafts from mice expressing ChR2 in pericytes were perfused with 4% PFA and organs were dissected, fixed overnight in 4% PFA, cryoprotected in a sucrose gradient (10, 20 and 30% w/w sucrose), and frozen in Tissue-Tek Optimal Cutting Temperature (OCT) compound before cryosectioning (-20°C). After a rinse with PBS-Triton X-100 (0.3%), sections were incubated in blocking solution (PBS-Triton X-100 and Universal Blocker Reagent; Biogenex, San Ramon, CA). Thereafter, sections were incubated 48 h with primary antibodies diluted in blocking solution. We immunostained beta cells (insulin; Accurate Chemical & Scientific, Wesbury, NY), sympathetic nerves (tyrosine hydroxylase), endothelial cells (PECAM; BD Biosciences, San Jose, CA), and pericytes with antibodies against different markers: neuron-glia antigen 2 (NG2; Millipore), PDGFR β (AF385-R&D Systems) and CD146. tdTomato was used as a reporter of ChR2 expression and amplified with an antibody against mCherry. Immunostaining was visualized by using Alexa Fluor conjugated secondary antibodies (1:500 in PBS; 16 hr; Invitrogen, Carlsbad, CA). Pimonidazole is reductively activated in hypoxic cells and forms stable adducts that can be detected with a fluorescent antibody (FITC-Mab1; HypoxyprobeTM). Cell nuclei were stained with DAPI. Slides were mounted with Vectashield mounting medium (Vector Laboratories) and imaged on a confocal microscope. ImageJ was used to quantify endocrine and vascular cell numbers in confocal planes. To determine colocalization between pericyte markers NG2, PDGFR β and CD146 and ChR2 (tdTomato), we used the ImageJ plugin “intensity correlation analysis” and calculated the Mander’s Colocalization coefficients (M1 and M2). These coefficients avoid issues related to the absolute intensities of the signals, since they are normalized against total pixel intensity (8), and represent the fraction of NG2 that is present in ChR2/tdTomato positive structures (M1) and vice –versa (M2). Quantifications were performed in confocal images, in a minimum of 3 islet/grafts per mice/3 mice per group.

Supplementary Table 1. Characteristics of human donors used in this study.

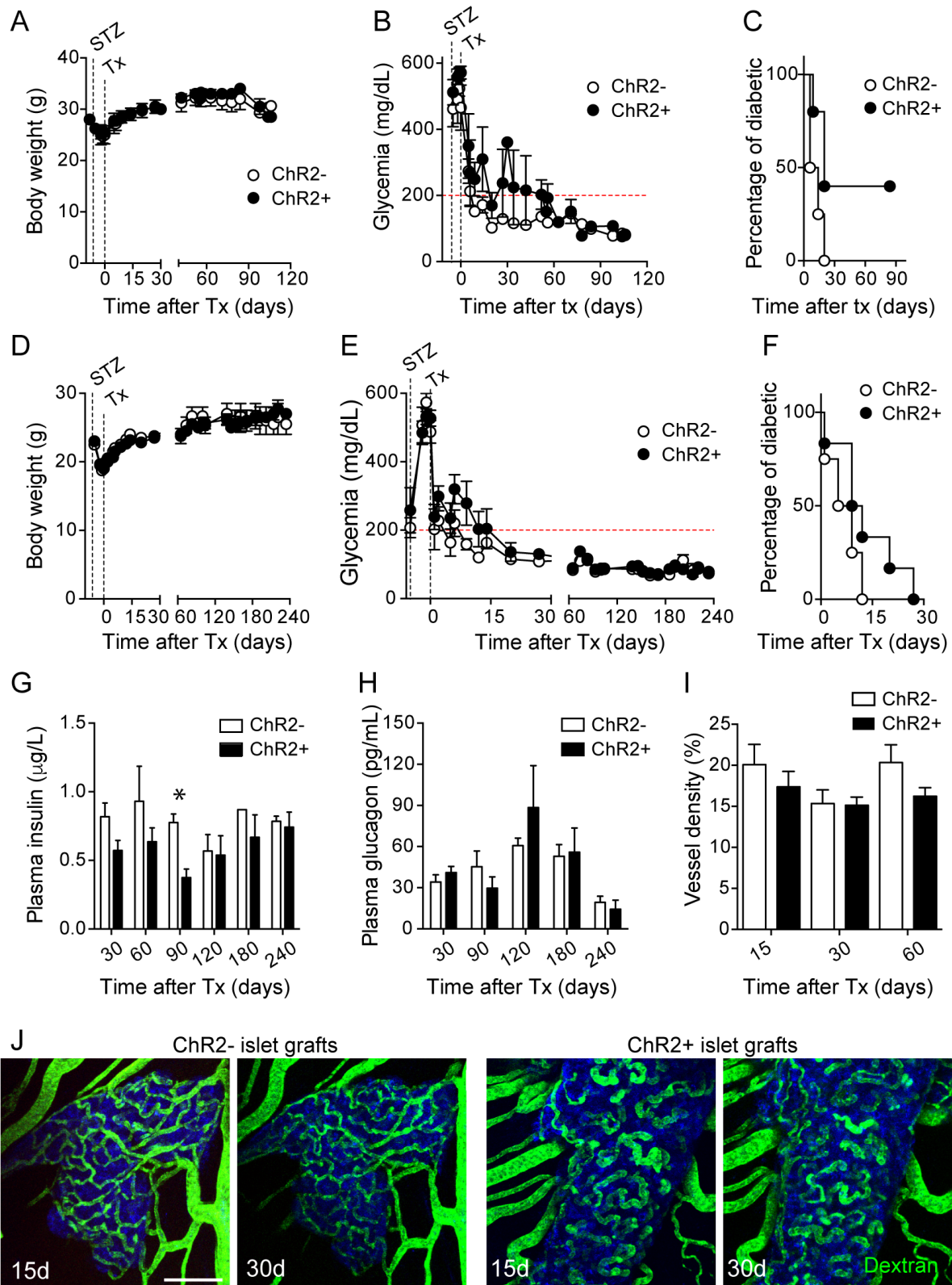
We obtained living human pancreas slices from de-identified cadaveric donors (from the head of the pancreas) from the Network of Pancreatic Organ Donors with Diabetes (nPOD). Slices produced by nPOD were shipped overnight from Gainesville to Miami and used in physiological experiments 3h after arrival.

CaseID	Donor Type	AutoAb (RIA)	Age (yrs)	Gender	Ethnicity	C-pep (ng/ml)	HbA1c	BMI
6516	No diabetes	Negative	20.75	Male	Caucasian	8.91	5.5	28.8
6531	No diabetes	Negative	19.25	Female	Hispanic	26.53	5.5	30
6535	No diabetes	Negative	31.07	Female	Caucasian	6.59		29.6
6537	No diabetes	Negative	33.05	Male	Caucasian	0.32	5.6	20.8
6539	No diabetes	Negative	24.6	Male	Hispanic	39.23	5.7	19.3
6546	No diabetes	Negative	22.29	Male	Asian	11	5.6	23.7
6548	No diabetes	Negative	20.24	Male	Caucasian	4.04	5.7	23.8

Supplementary Figures

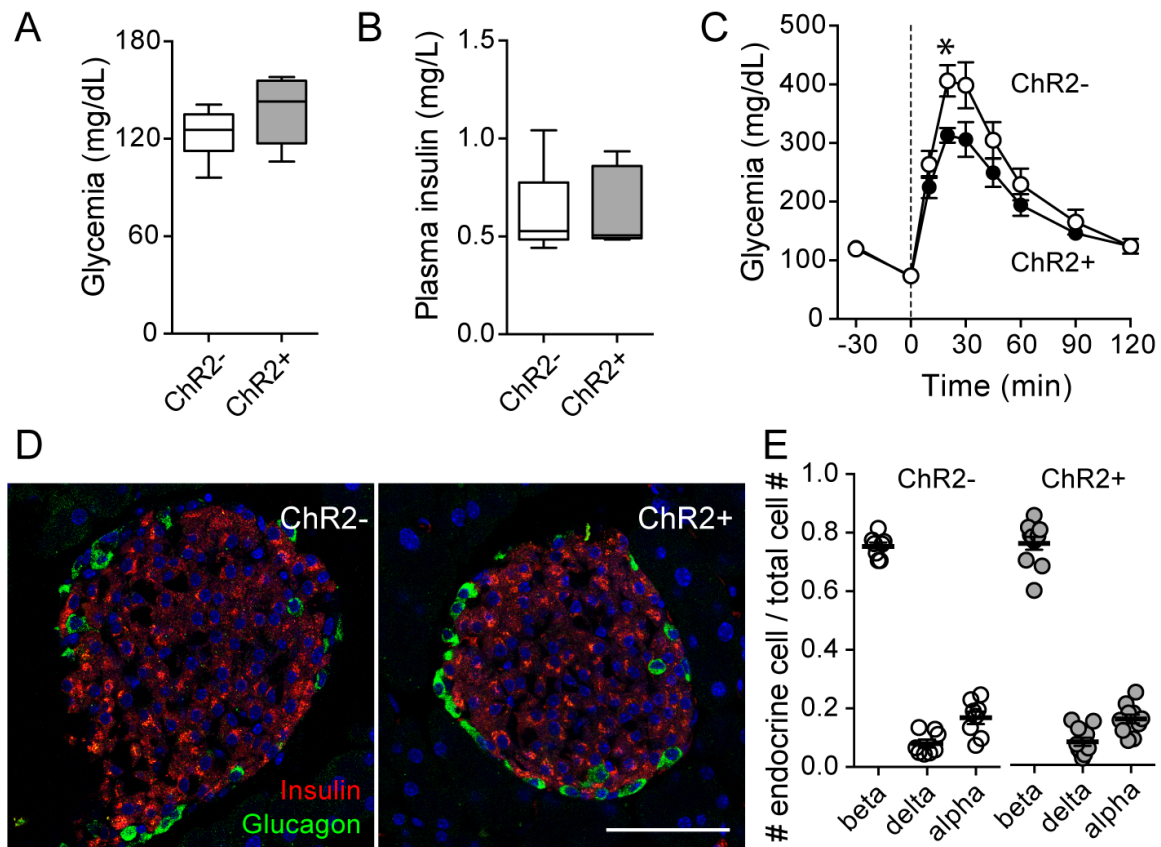


Supplementary Figure 1. Blood vessels in human pancreatic islets are enriched with pericytes. A, Maximal projection of confocal images of the same human islet in a pancreas section immunostained for insulin (red) and the mural cell markers NG2 (green, left panel) and alpha smooth muscle actin (α SMA, green, right panel). **B, B'** Zoomed images of regions within dashed rectangles in (A) showing differential morphology and expression of NG2 and α SMA of islet pericytes (B) and vascular smooth muscle cells (B'). C, D, Maximal projection of confocal images of human islets in sections immunostained for insulin (red) and platelet-derived growth factor receptor β (PDGFR β , green; C) or for NG2 (green) and PDGFR β (red, D). E, F, Maximal projection of confocal images of a human islet in a section immunostained for insulin (red) and CD146 (green, E) or NG2 (green) and CD146 (red, F). Note that NG2-expressing pericytes in human islets also express PDGFR β and CD146, and around 50% of them expresses α SMA as previously reported (1, 2). However, expression of α SMA, PDGFR β and CD146 is not limited to pericytes in islets in the human pancreas. Scale bars = 50 μ m (A, C, E), 20 μ m (B, D, F).



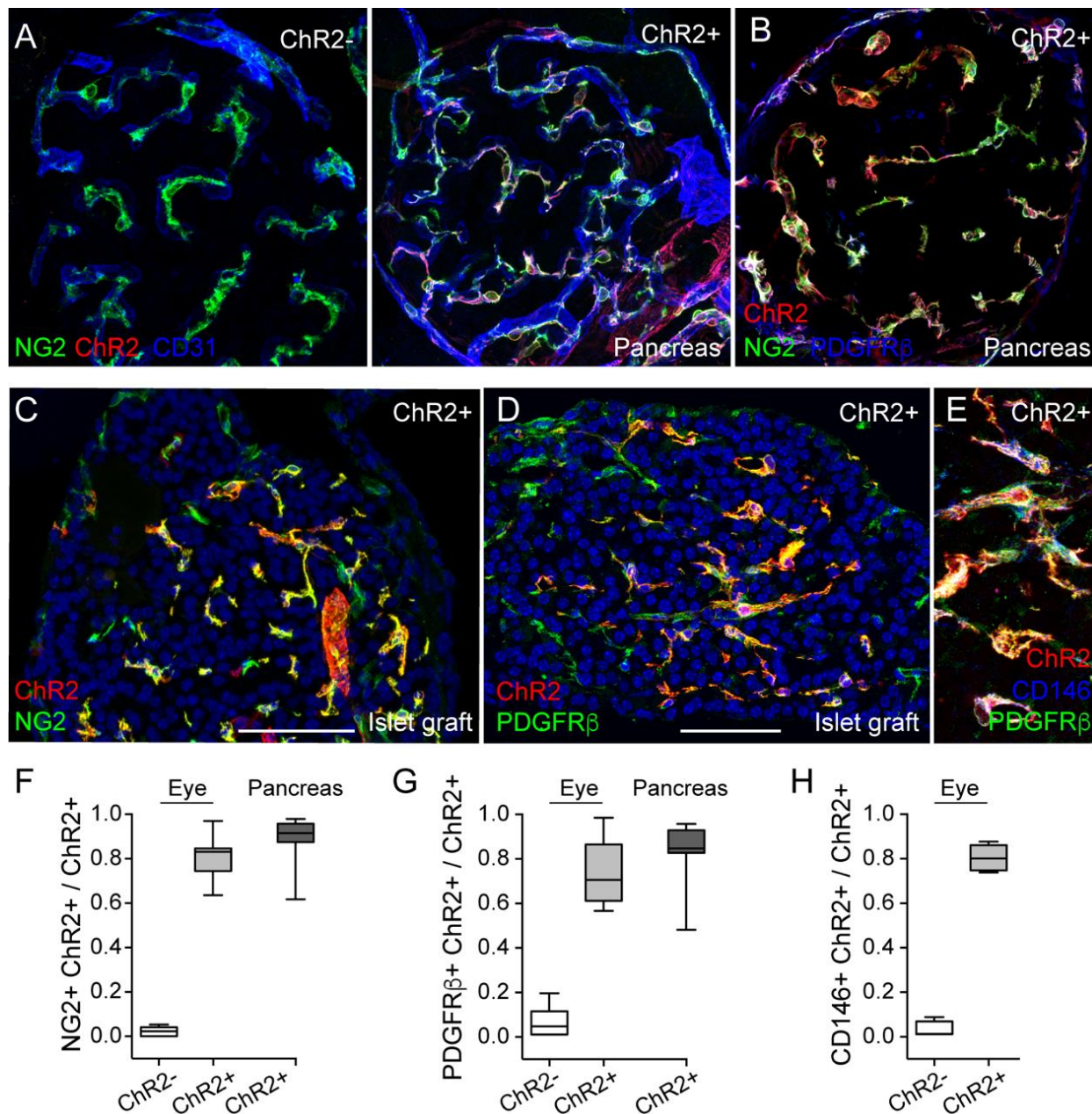
Supplementary Figure 2. Islets from NG2-ChR2+ mice get revascularized and take control of glucose metabolism in transplanted animals. A-F, To assess the effects

on glucose metabolism of selective activation of islet pericytes, we transplanted islets from mice that express ChR2 in pericytes (ChR2+) into the eyes of male (A-C; n=5) and female (D-F; n=6) Nude mice (3 months old). As control, we also transplanted islets from mice that do not express ChR2 in pericytes (ChR2-; n=4 male and 4 female recipients). Male and female Nude mice were rendered diabetic (with a STZ injection) before islet transplantation. Islet transplantation reversed hyperglycemia in all the animals that received ChR2- islets (n=8 pooled genders), and in 9 out of 11 mice that received ChR2+ islets (both animals that did not become normoglycemic after transplantation were males; (C)). Mice increased their body weight when normoglycemia was achieved suggesting full recovery from STZ treatment. G,H, Measurements of non-fasting plasma insulin and glucagon at different time points after transplantation. I,J, To monitor the engraftment process, we followed islet revascularization longitudinally by imaging the eye at different time points after transplantation. Animals were injected intravenously with a fluorescent dextran (green). Vessel density in NG2-ChR2+ and NG2-ChR2- grafts at different time points was similar. Scale bar = 50 μ m (J).



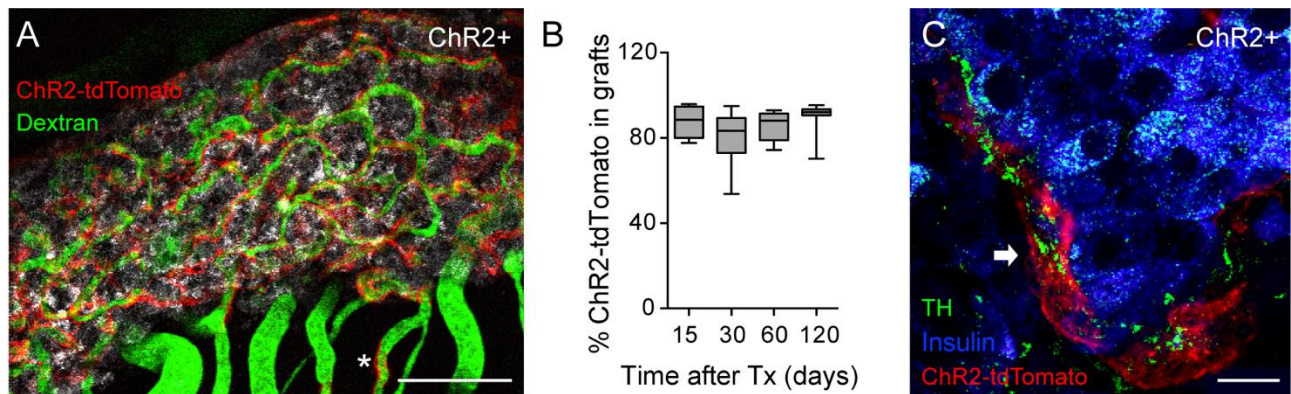
Supplementary Figure 3. Glucose metabolism and islet endocrine cell

composition in NG2-ChR2⁺ donor mice. A, Pericytes are excitable cells whose contractile activity requires changes in cytosolic calcium levels (9). To manipulate their activity, we generated mice that express the blue light sensitive ion channel channelrhodopsin2 in pericytes using the Cre/Lox system (see Methods). We generated mice that express ChR2 in pericytes (Cre⁺; ChR2⁺) and mice that do not express ChR2 in pericytes (Cre⁻; ChR2⁻). Fed glycemia (A) and plasma insulin levels (B) were not different between donor ChR2⁺ and ChR2⁻ mice at 3 months of age. C, Glucose tolerance was slightly better in ChR2⁺ mice. D,E, Endocrine cells were visualized with antibodies against insulin (beta cells; red), glucagon (alpha cells; green) and somatostatin (delta cells). Islet cytoarchitecture (D) and proportion of different endocrine cells (E) was not different between ChR2⁻ and ChR2⁺ donor mice. Scale bar = 50 μ m (D).

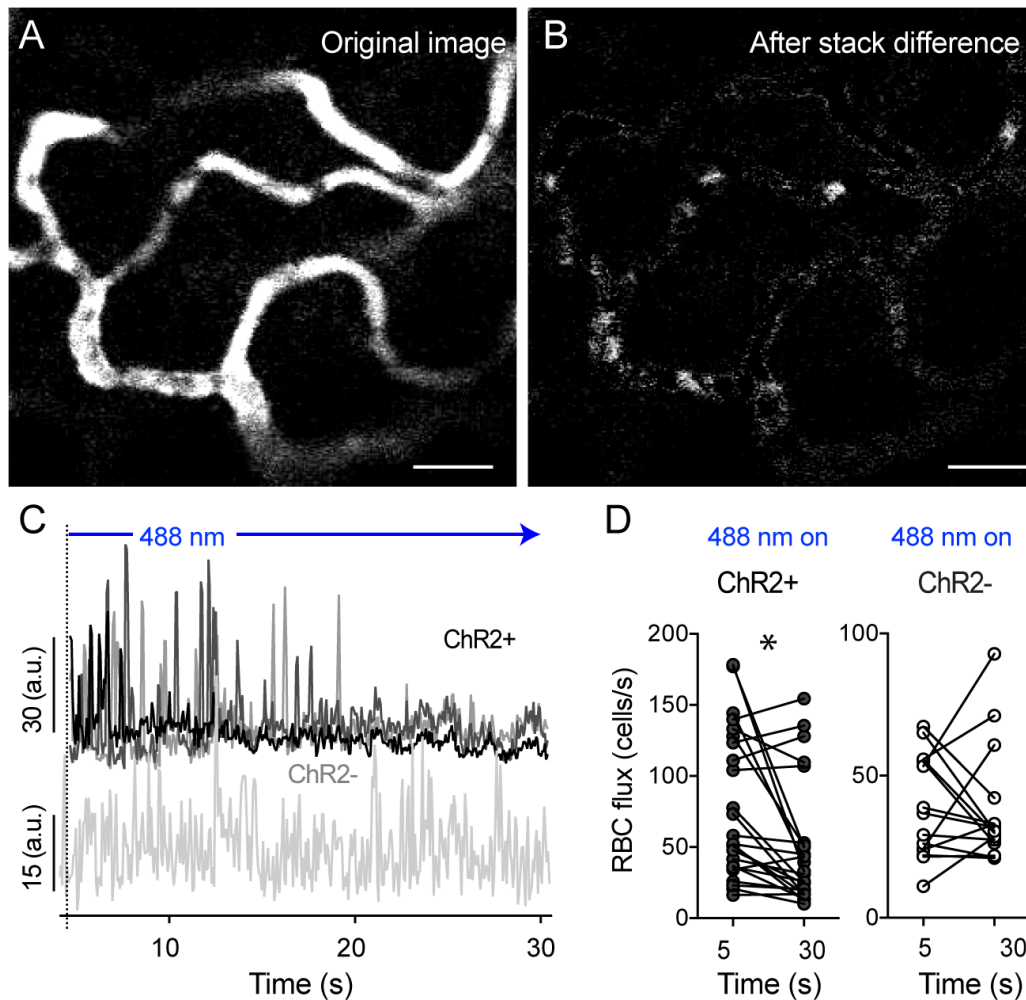


Supplementary Figure 4. ChR2 is expressed by pericytes in the pancreas and in intraocular islet grafts after revascularization. A,B, Maximal projection of confocal images of islets in pancreatic sections of NG2-ChR2⁻ and NG2-ChR2⁺ mice immunostained for tdTomato (ChR2, red), pericytes (NG2, green) and either endothelial cells (CD31, blue; A) or PDGFR β (blue; B). ChR2 is expressed by islet pericytes in ChR2⁺ mice, but not in ChR2⁻ mice. C-E, Maximal projection of confocal images of intraocular islet grafts of NG2-ChR2⁺ mice immunostained for tdTomato (ChR2, red) and different pericyte markers such as NG2 (green; C), PDGFR β (green; D) and CD146

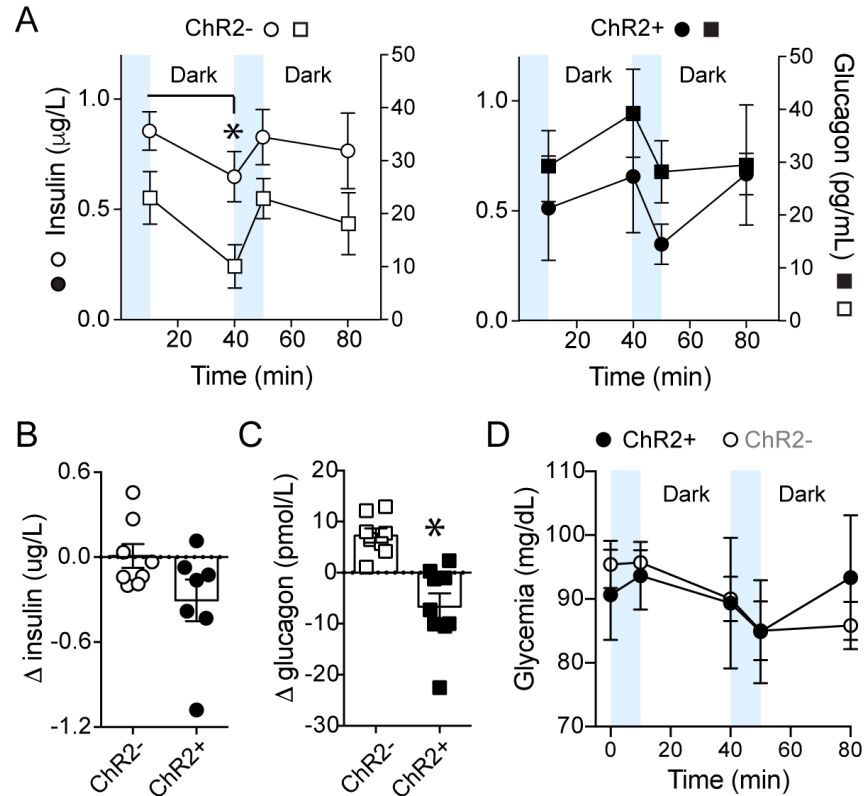
(blue; E). In (E) PDGFR β is shown in green. Scale bars = 50 μ m. F-H, Mander's M1 coefficients reflecting colocalization of tdTomato (ChR2) with NG2 (F), PDGFR β (G) and CD146 (H) for islets in the pancreas and in intraocular islet grafts of NG2-ChR2- and NG2-ChR2+ mice. tdTomato (ChR2) is almost exclusively expressed by islet pericytes in the pancreas and in the eye.



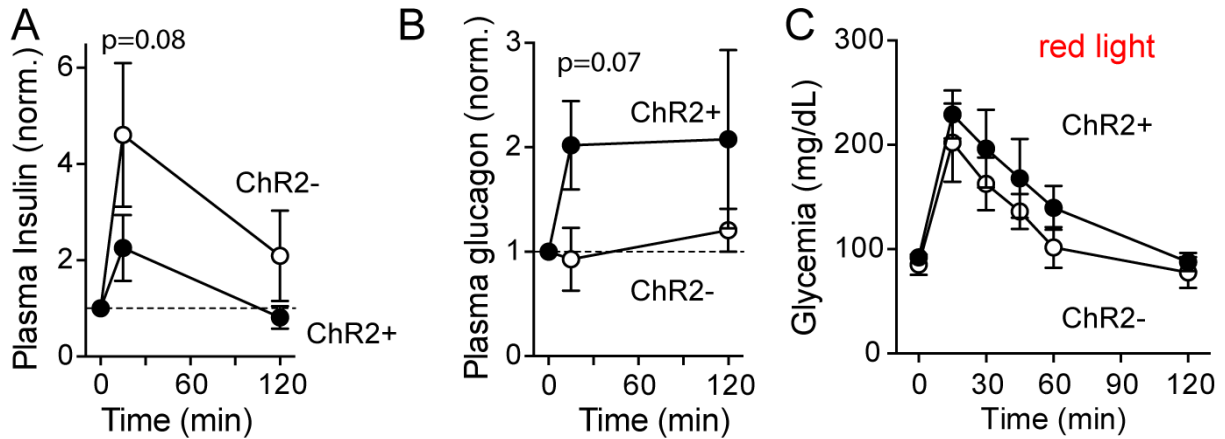
Supplementary Figure 5. ChR2-expressing pericytes remain associated with capillaries and receive sympathetic innervation in islet grafts after transplantation. A, ChR2 expressing pericytes (red) and blood vessels (dextran labeled, green) in intraocular islet grafts from NG2-ChR2+ mice can be visualized *in vivo* after transplantation. * indicates one pericyte that has left the islet graft and is associated with the iris vasculature. B, Quantification of the percentage of tdTomato (ChR2) fluorescence that is associated with regions with backscatter (islet grafts). 80-90% of tdTomato expressing cells are in islet grafts. C, Sympathetic nerves (tyrosine hydroxylase (TH)-positive, green) regrow after transplantation and revascularization of intraocular islet grafts (10). Three months after transplantation, sympathetic nerves in intraocular islet grafts contact ChR2-expressing pericytes (red; arrow). Insulin is shown in blue. Scale bar = 50 μ m (A) and 10 μ m (C).



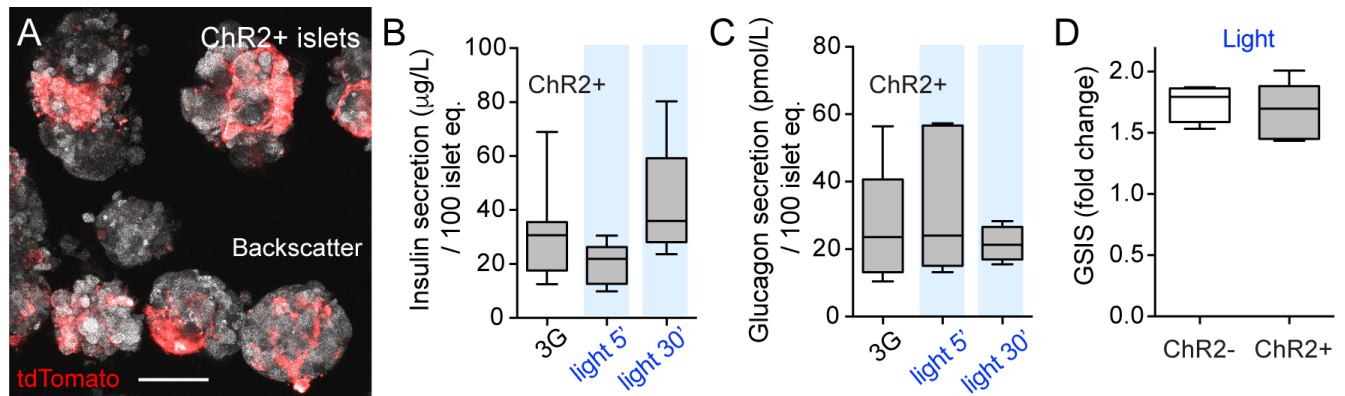
Supplementary Figure 6. Pericyte activation with optogenetics decreases blood flow in islet graft capillaries. A, Confocal image of red blood cells flowing through capillaries in an islet graft from NG2-ChR2⁺ mice. B, Corresponding image after applying the "Stack Difference" ImageJ plugin to detect dynamic changes (that reflect RBC movement). C, Traces showing changes in fluorescence in ROIs placed on different capillaries in islet grafts from NG2-ChR2⁺ and NG2-ChR2⁻ mice after performing stack difference. Changes in fluorescence originate from RBC movement through vessels. The area under the curve of fluorescence traces was calculated every 5 sec to estimate RBC flux (total amount of cells moving/time). D, Values of RBC fluxes at 5 and 30 sec after stimulation with 488 nm laser in capillaries in ChR2⁺ and ChR2⁻ islet grafts. There is a significant decrease in RBC flux in ChR2⁺ graft capillaries but not in ChR2⁻ capillaries (paired t-test, $p=0.004$, $n=24$ vessels/3mice). Scale bars = 20 μm .



Supplementary Figure 7. Pericyte activation with blue light overcomes the effects of autonomic input on islet grafts in the context of the pupillary light reflex. A, Acute exposure of transplanted animals to blue light (10 min) increased plasma insulin (circles) and glucagon (squares) secretion in control mice (NG2-ChR2⁻; white symbols; left panel; n = 3 mice) but decreased both hormones in mice with ChR2 expressing islet pericytes (NG2-ChR2⁺; black symbols; right panel; n = 3 mice). B,C, Shown is the difference (Δ) between hormone levels at the beginning and end of the second 10 min-period of chronic stimulation with blue light (*p < 0.05, unpaired Student's t-test, n = 7-8 mice). D, Accompanying changes in glycemia in transplanted animals placed in the dark and subjected to 10 min interval of blue light stimulation (n = 7-8 mice).

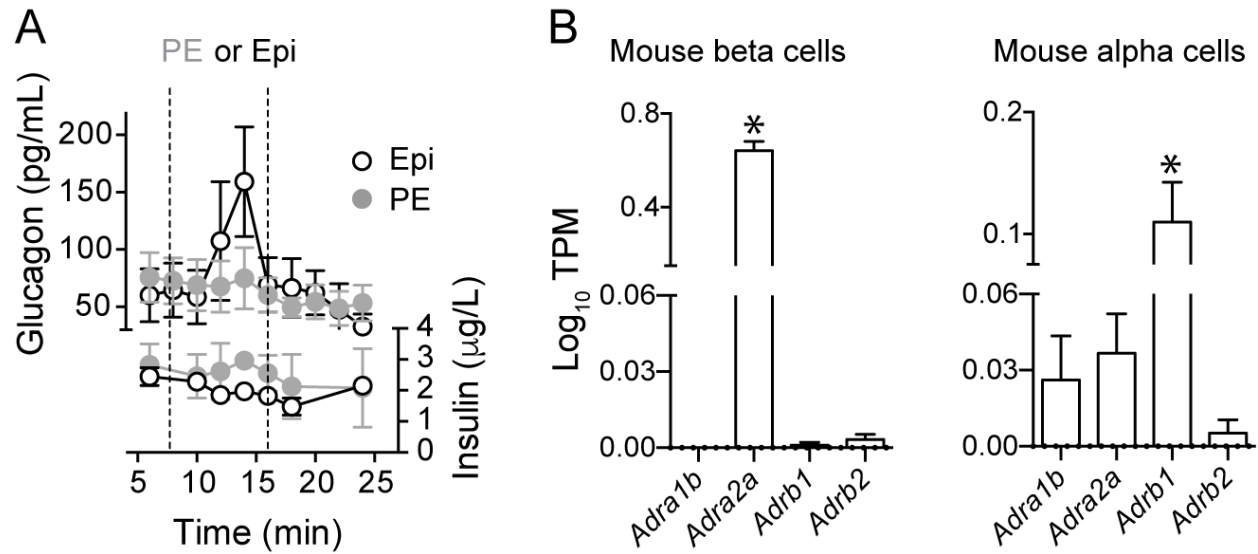


Supplementary Figure 8. Red light does not affect glucose tolerance in transplanted mice. A,B, Changes in plasma insulin (A) and glucagon (B) induced by glucose (i.p.) in NG2-ChR2+ (black) and NG2-ChR2- mice (white), normalized to values at t = 0 min (One sample t-test; $p > 0.05$ for ChR2+ compared to a theoretical mean of 1). C, Glucose excursions of an intraperitoneal glucose tolerance test (IPGTT) performed in awake, freely moving mice transplanted with islets from NG2-ChR2+ (black) and NG2-ChR2- mice (white) in the presence of red light pulses (1 min on, 4 min off; light pulses started 1h before and continued during the IPGTT; $n = 7-9$ mice/group).

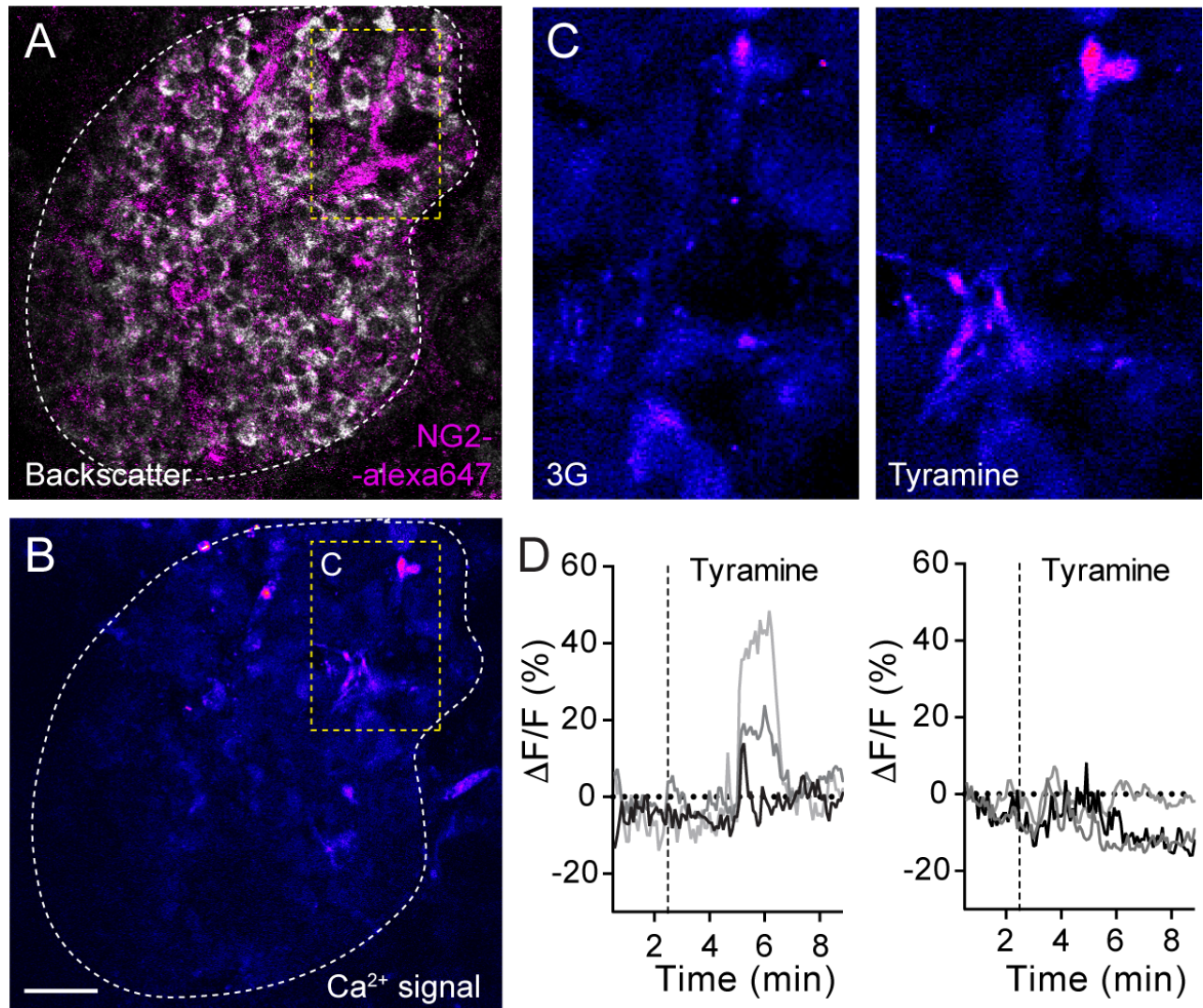


Supplementary Figure 9. Optogenetic activation of pericytes *in vitro* does not affect islet hormone secretion.

A, Islets were isolated from NG2-ChR2+ and NG2-ChR2- mice. Maximal projection of confocal images of NG2-ChR2+ isolated islets showing that ChR2-expressing pericytes remain in islets after 24h in culture. Isolated islets were stimulated *in vitro* at 37°C with blue light for 5 or 30 min in 3 mM glucose buffered solution (3G; B,C) or in 16 mM glucose solution for 45 min (D). B,C, Effect of blue light on insulin (B) and glucagon secretion (C) in 3 mM glucose ($p > 0.05$, One-way ANOVA Tukey's multiple comparisons test, $n = 5$). D, Fold change in the amount of insulin that was secreted upon changing extracellular glucose from 3 mM to 16 mM from NG2-ChR2+ or NG2-ChR2- islets in the presence of blue light ($p > 0.05$, unpaired t-test, $n = 5$). Scale bar = 100 μ m.



Supplementary Figure 10. *In vitro* responses to adrenergic stimulation and adrenergic receptor expression in mouse islets. A, Changes in insulin and glucagon secretion from isolated mouse islets *in vitro* induced by PE (10 μ M) or epinephrine (10 μ M). Both stimuli were applied in 3 mM glucose. PE has no effect on insulin or glucagon secretion *in vitro*, while epinephrine stimulates glucagon secretion and inhibits insulin secretion from isolated mouse islets. B, Single-cell RNA seq data showing transcripts levels encoding different adrenergic receptors expressed by mouse alpha or beta cells. Shown are log₁₀ transcripts per million (TPM) values that were taken from Baron et al. [(11);*p<0.05, One-way ANOVA followed by Tukey's multiple comparisons test].



Supplementary Figure 11. A subset of pericytes in human islets responds to tyramine. A,B, Living human pancreas slices were incubated with a fluorescent antibody against NG2 (NG2-alexa647, magenta) and with a membrane permeant Ca^{2+} indicator (Fluo4) for $[\text{Ca}^{2+}]_i$ imaging (pseudo color scale, B). C, Zoomed images of region within dashed yellow rectangle (in A and B) showing cellular responses to tyramine (100 μM) in 3 mM glucose containing extracellular solution (3G). D, Traces showing changes in $[\text{Ca}^{2+}]_i$ in islet pericytes induced by tyramine. Not all islet pericytes show an increase in $[\text{Ca}^{2+}]_i$ upon tyramine stimulation.

Supplementary Movies

Supplementary Movie 1. Constriction of islet capillaries induced by optogenetic activation of pericytes. Movie composed of a series of confocal images taken every 68 msec of ChR2-expressing pericytes (red) in an islet graft in the eye. Endocrine cells are seen in gray (backscattered light). Turning on the 488 nm laser leads to a constriction of the islet vessel indicated with an asterisk. Note that constriction is reversible and, when the laser is turned off, blood flow through that capillary resumes. Movie speed 40 frames per second (fps).

Supplementary Movie 2. Optogenetic activation of islet pericytes decreases blood flow in intraocular islet graft capillaries. Movie composed of a series of confocal images taken every 68 msec of islet capillaries (labeled with a dextran, green) covered by ChR2-expressing pericytes (red) in an intraocular graft from a NG2-ChR2+ mice. Endocrine cells are seen in blue (backscattered light). Turning on the 488 nm laser allows us to visualize vessels and leads to a decrease in islet blood flow in some capillaries in the graft. Note that blood flow completely stops in the capillary in the middle of the graft shown with an asterisk. Movie speed 20 frames per second (fps).

Supplementary Movie 3. Optogenetic activation of islet pericytes decreases blood flow in intraocular islet graft capillaries. Movie composed of a series of confocal images taken every 68 msec of ChR2-expressing pericytes (red) covering islet capillaries (labeled with a dextran, green) in an intraocular graft from NG2-ChR2+ mice. Endocrine cells are seen in blue (backscattered light). Turning on the 488 nm laser allows us to visualize the vessels and leads to a decrease in islet blood flow in some vessels in the graft. Note that blood flow completely stops in some vessels. Changes are reversible and blood starts flowing again shortly after turning off the 488 nm laser. Movie speed 40 frames per second (fps).

Supplementary Movie 4. Optogenetic activation of islet pericytes decreases blood flow in intraocular islet graft capillaries. Movie composed of a series of confocal images taken every 68 msec of ChR2-expressing pericytes (red) covering islet capillaries (labeled with a dextran, green) in an intraocular graft from NG2-ChR2+ mice. Endocrine cells are seen in blue (backscattered light). Turning on the 488 nm laser allows us to visualize the vessels and leads to a decrease in islet blood flow in some vessels in the graft (some responsive vessels are indicated with *). Note that blood flow completely stops in some vessels. Movie speed 40 frames per second (fps).

Supplementary References

1. Mateus Gonçalves L & Almaça J (2020) Functional Characterization of the Human Islet Microvasculature Using Living Pancreas Slices. *Frontiers in endocrinology* 11:602519.
2. Almaça J, Weitz J, Rodriguez-Diaz R, Pereira E, & Caicedo A (2018) The Pericyte of the Pancreatic Islet Regulates Capillary Diameter and Local Blood Flow. *Cell metabolism* 27(3):630-644 e634.
3. Speier S, *et al.* (2008) Noninvasive in vivo imaging of pancreatic islet cell biology. *Nature medicine* 14(5):574-578.
4. Almaça J, *et al.* (2014) Young capillary vessels rejuvenate aged pancreatic islets. *Proceedings of the National Academy of Sciences of the United States of America* 111(49):17612-17617.
5. Santoso F, *et al.* (2019) Development of a Simple ImageJ-Based Method for Dynamic Blood Flow Tracking in Zebrafish Embryos and Its Application in Drug Toxicity Evaluation. *Inventions* 4(65).
6. D'Hoker J, *et al.* (2013) Conditional hypovascularization and hypoxia in islets do not overtly influence adult β -cell mass or function. *Diabetes* 62(12):4165-4173.
7. Seckler JM, *et al.* (2020) NADPH diaphorase detects S-nitrosylated proteins in aldehyde-treated biological tissues. *Scientific reports* 10(1):21088.
8. Manders EMM, Verbeek FJ, & Aten JA (1993) Measurement of co-localization of objects in dual-colour confocal images. *Journal of Microscopy* 169(3):375-382.
9. Burdyga T & Borysova L (2014) Calcium signalling in pericytes. *Journal of vascular research* 51(3):190-199.
10. Rodriguez-Diaz R, *et al.* (2012) Noninvasive in vivo model demonstrating the effects of autonomic innervation on pancreatic islet function. *Proceedings of the National Academy of Sciences of the United States of America* 109(52):21456-21461.
11. Baron M, *et al.* (2016) A Single-Cell Transcriptomic Map of the Human and Mouse Pancreas Reveals Inter- and Intra-cell Population Structure. *Cell systems* 3(4):346-360.e344.